New complex variable meshless method for advection–diffusion problems*

Wang Jian-Fei(王健菲) and Cheng Yu-Min(程玉民)†

Shanghai Institute of Applied Mathematics and Mechanics, Shanghai University, Shanghai 200072, China
Shanghai Key Laboratory of Mechanics in Energy Engineering, Shanghai University, Shanghai 200072, China

(Received 13 August 2012; revised manuscript received 27 August 2012)

In this paper, an improved complex variable meshless method (ICVMM) for two-dimensional advection–diffusion problems is developed based on improved complex variable moving least-square (ICVMLS) approximation. The equivalent functional of two-dimensional advection–diffusion problems is formed, the variation method is used to obtain the equation system, and the penalty method is employed to impose the essential boundary conditions. The difference method for two-point boundary value problems is used to obtain the discrete equations. Then the corresponding formulas of the ICVMM for advection–diffusion problems are presented. Two numerical examples with different node distributions are used to validate and investigate the accuracy and efficiency of the new method in this paper. It is shown that ICVMM is very effective for advection–diffusion problems, and has a good convergent character, accuracy, and computational efficiency.

Keywords: meshless method, improved complex variable moving least-square approximation, improved complex variable meshless method, advection–diffusion problem

PACS: 02.60.Cb, 02.60.Lj, 66.10.C–, 82.56.Lz **DOI:** 10.1088/1674-1056/22/3/030208

1. Introduction

The advection–diffusion problem is important to many branches of science and engineering. Many physical and chemical phenomena, such as the diffusion of polluted substances in water and air, the diffusion of heat and salinity in the ocean, even economics and financial forecasting, can be described as advection–diffusion problems. In recent years, the finite difference method, finite volume method, and finite element method for advection–diffusion problems have been developed.[1–5]

Depending on the values of the advection and diffusion coefficients, the advection–diffusion problem becomes parabolic for a diffusion-dominated process and hyperbolic for an advection-dominated process.[6] Traditional methods are generally accurate for solving the former but not the latter because oscillations and dampings are introduced.[7–9] Developing stable and accurate numerical methods for advection–diffusion problems is therefore quite challenging.

Because of the complexity of mesh-generation, considerable effort has been devoted to the development of meshless methods, which have developed so fast that they are now applied successfully to many fields of science and engineering.[10–18]

Among the meshless methods, the moving least-square (MLS) approximation is one of the most widely used method to construct the shape function.[19] It has been found that this method is accurate and stable for arbitrarily distributed nodes in many problems. To improve its computational efficiency, improved complex variable moving least-square (ICVMLS) approximation was discussed,[20] and its functional has an explicit physical meaning, which is also an advantage over the complex variable moving least-square (CVMLS) approximation[21] and the MLS approximation.[22] The ICVMLS approximation is the approximation of a vector function, and thus the trial function of two-dimensional problems can be formed with a one-dimensional basis function. Therefore, the number of unknown coefficients in the trial function of the ICVMLS approximation is less than that of the MLS approximation, and we can select fewer nodes in the meshless method developed from ICVMLS approximation with no loss of precision.

In this paper, based on the improved complex variable moving least-square approximation, an improved complex variable meshless method (ICVMM) for two-dimensional advection–diffusion problems is developed. The numerical examples show that ICVMM is very effective for advection–diffusion problems, and has a good convergent character, accuracy, and computational efficiency.

2. Improved complex variable moving least-square approximation

In the ICVMLS approximation, the function $u(z)$ is approximated by $u^{\mathrm{h}}(z)$, which can be defined by

$$u^{\mathrm{h}}(z) = u_1^{\mathrm{h}}(z) + \mathrm{i}u_2^{\mathrm{h}}(z) = \sum_{i=1}^{m} \bar{p}_i(z)a_i(z) = \bar{\boldsymbol{p}}^T(z)\boldsymbol{a}(z),$$

*Project supported by the National Natural Science Foundation of China (Grant No. 11171208), the Shanghai Leading Academic Discipline Project, China (Grant No. S30106), and the Innovation Fund for Graduate Student of Shanghai University, China (Grant No. SHUCX120125).

†Corresponding author. E-mail: ymcheng@shu.edu.cn

© 2013 Chinese Physical Society and IOP Publishing Ltd

$$z = x_1 + \mathrm{i}x_2 \in \Omega, \tag{1}$$

where $\bar{\boldsymbol{p}}^{\mathrm{T}}(z) = (\bar{p}_1(z), \bar{p}_2(z), \ldots, \bar{p}_m(z))$ is the basis function vector which equals the conjugate of basis function vector $\boldsymbol{p}^{\mathrm{T}}(z) = (p_1(z), p_2(z), \ldots, p_m(z))$, $\boldsymbol{a}^{\mathrm{T}}(z) = (a_1(z), a_2(z), \ldots, a_m(z))$ is the corresponding coefficient vector, and m is the number of terms in the basis function vector.

The local approximation at point z is defined as

$$u^{\mathrm{h}}(z, \hat{z}) = \sum_{i=1}^{m} \bar{p}_i(\hat{z}) a_i(z) = \bar{\boldsymbol{p}}^{\mathrm{T}}(\hat{z}) \boldsymbol{a}(z), \tag{2}$$

where $\hat{z}$ represents the nodes in the local support domain of z, and $a_i(z)$ $(i = 1, 2, \ldots, m)$ are determined by minimizing the following functional.

Define a functional

$$\begin{aligned} J &= \sum_{I=1}^{n} w(z - z_I) \left| u^{\mathrm{h}}(z, z_I) - u(z_I) \right|^2 \\ &= \sum_{I=1}^{n} w(z - z_I) \left(\sum_{i=1}^{m} \bar{p}_i(z_I) \cdot a_i(z) - u(z_I) \right) \\ &\quad \times \overline{\left(\sum_{i=1}^{m} \bar{p}_i(z_I) \cdot a_i(z) - u(z_I) \right)}, \end{aligned} \tag{3}$$

where $w(z - z_I)$ is a weight function with compact support, z_I $(I = 1, 2, \ldots, n)$ are the nodes in the compact support domain of point z and

$$u(z_I) = u_1(z_I) + \mathrm{i}u_2(z_I). \tag{4}$$

For functions $f(z)$ and $g(z)$, we define the inner product as

$$(f, g)_z = \sum_{I=1}^{n} w(z - z_I) f(z_I) \bar{g}(z_I), \quad \forall f, g \in C^0(\bar{\Omega}), \tag{5}$$

where $\bar{g}(z_I)$ is the conjugate of $g(z_I)$, $\bar{\Omega} = \Omega \cup \partial\Omega$, and $C^0(\bar{\Omega})$ is the set of all continuous functions in the domain $\bar{\Omega}$. Correspondingly, the norm is

$$||f||_z = [(f, f)_z]^{1/2}. \tag{6}$$

Equation (3) can be represented as

$$\begin{aligned} J &= (\bar{\boldsymbol{P}}\boldsymbol{a}(z) - \boldsymbol{u}^*(z))^{\mathrm{T}} \boldsymbol{W}(z) \overline{(\bar{\boldsymbol{P}}\boldsymbol{a}(z) - \boldsymbol{u}^*(z))} \\ &= \left\| \bar{\boldsymbol{p}}^{\mathrm{T}}(z) \cdot \boldsymbol{a}(z) - u \right\|_z^2, \end{aligned} \tag{7}$$

where

$$\bar{\boldsymbol{P}} = \begin{bmatrix} \bar{p}_1(z_1) & \bar{p}_2(z_1) & \ldots & \bar{p}_m(z_1) \\ \bar{p}_1(z_2) & \bar{p}_2(z_2) & \ldots & \bar{p}_m(z_2) \\ \vdots & \vdots & \ddots & \vdots \\ \bar{p}_1(z_n) & \bar{p}_2(z_n) & \ldots & \bar{p}_m(z_n) \end{bmatrix}_{n \times m}, \tag{8}$$

$$\boldsymbol{W}(z) = \begin{bmatrix} w(z - z_1) & 0 & \ldots & 0 \\ 0 & w(z - z_2) & \ldots & 0 \\ \vdots & \vdots & \ddots & \vdots \\ 0 & 0 & \ldots & w(z - z_n) \end{bmatrix}, \tag{9}$$

$$\boldsymbol{u}^* = (u(z_1), u(z_2), \ldots, u(z_n))^{\mathrm{T}} = \boldsymbol{Q}\boldsymbol{u}, \tag{10}$$

$$\boldsymbol{u} = (u_1(z_1), u_2(z_1), u_1(z_2), u_2(z_2), \ldots, u_1(z_n), u_2(z_n))^{\mathrm{T}}, \tag{11}$$

$$\boldsymbol{Q} = \begin{bmatrix} 1 & \mathrm{i} & 0 & 0 & 0 & 0 & \ldots & 0 & 0 \\ 0 & 0 & 1 & \mathrm{i} & 0 & 0 & \ldots & 0 & 0 \\ 0 & 0 & 0 & 0 & 1 & \mathrm{i} & \ldots & 0 & 0 \\ \vdots & \vdots & \vdots & \vdots & \vdots & \vdots & \ddots & \vdots & \vdots \\ 0 & 0 & 0 & 0 & 0 & 0 & \ldots & 1 & \mathrm{i} \end{bmatrix}_{n \times 2n}. \tag{12}$$

Equation (3) can be also written as

$$J = \left\| a_1\bar{p}_1 + a_2\bar{p}_2 + \ldots + a_m\bar{p}_m - u \right\|_z^2, \tag{13}$$

where $\bar{p}_i = \bar{p}_i(z)$, $i = 1, 2, \ldots, m$.

Let $u^{(1)}$ be the projection of u in the span$(\bar{p}_1, \bar{p}_2, \ldots, \bar{p}_m)$, obviously,

$$J^{(1)} = \left\| u^{(1)} - u \right\|_z^2 \tag{14}$$

is the minimum of functional J.

The function u could be decomposed orthogonally into

$$u = u^{(1)} + u^{(2)}, \tag{15}$$

where $u^{(2)} \perp \mathrm{span}(\bar{p}_1, \bar{p}_2, \ldots, \bar{p}_m)$. Obviously,

$$(\bar{p}_i, u^{(2)})_z = 0, \quad (i = 1, 2, \ldots, m), \tag{16}$$

then we obtain

$$\begin{aligned} (\bar{p}_i, u)_z &= (\bar{p}_i, u^{(1)})_z + (\bar{p}_i, u^{(2)})_z = (\bar{p}_i, u^{(1)})_z, \\ &\quad (i = 1, 2, \ldots, m), \end{aligned} \tag{17}$$

$$(\bar{p}_i, u)_z = (\bar{p}_i, u^{(1)})_z = (\bar{p}_i, a_1\bar{p}_1 + a_2\bar{p}_2 + \ldots + a_m\bar{p}_m)_z. \tag{18}$$

The matrix form of Eq. (18) is

$$\begin{aligned} &\begin{bmatrix} (\bar{p}_1, \bar{p}_1)_z & (\bar{p}_1, \bar{p}_2)_z & \ldots & (\bar{p}_1, \bar{p}_m)_z \\ (\bar{p}_2, \bar{p}_1)_z & (\bar{p}_2, \bar{p}_2)_z & \ldots & (\bar{p}_2, \bar{p}_m)_z \\ \vdots & \vdots & \ddots & \vdots \\ (\bar{p}_m, \bar{p}_1)_z & (\bar{p}_m, \bar{p}_2)_z & \ldots & (\bar{p}_m, \bar{p}_m)_z \end{bmatrix} \\ &\times \begin{bmatrix} \bar{a}_1(z) \\ \bar{a}_2(z) \\ \vdots \\ \bar{a}_m(z) \end{bmatrix} = \begin{bmatrix} (\bar{p}_1, u)_z \\ (\bar{p}_2, u)_z \\ \vdots \\ (\bar{p}_m, u)_z \end{bmatrix}, \end{aligned} \tag{19}$$

that is

$$(\bar{\boldsymbol{P}}^{\mathrm{T}} \boldsymbol{W}(z) \boldsymbol{P}) \bar{\boldsymbol{a}}(z) = \bar{\boldsymbol{P}}^{\mathrm{T}} \boldsymbol{W}(z) \bar{\boldsymbol{u}}^*. \tag{20}$$

The conjugate of Eq. (20) can be written as

$$(\boldsymbol{P}^{\mathrm{T}} \boldsymbol{W}(z) \bar{\boldsymbol{P}}) \boldsymbol{a}(z) = \boldsymbol{P}^{\mathrm{T}} \boldsymbol{W}(z) \boldsymbol{u}^*. \tag{21}$$

Solving Eq. (21) for $\boldsymbol{a}(z)$, we obtain

$$\boldsymbol{a}(z) = \boldsymbol{C}^{-1}(z) \boldsymbol{B}(z) \boldsymbol{u}^*, \tag{22}$$

where matrices $\boldsymbol{B}(z)$ and $\boldsymbol{C}(z)$ are defined by

$$\boldsymbol{B}(z) = \boldsymbol{P}^{\mathrm{T}} \boldsymbol{W}(z), \tag{23}$$

$$\boldsymbol{C}(z) = \boldsymbol{P}^{\mathrm{T}}\boldsymbol{W}(z)\bar{\boldsymbol{P}}. \tag{24}$$

Combining Eq. (22) with Eq. (2), we can write the final form of the local approximation $u^{\mathrm{h}}(z,\hat{z})$ as

$$u^{\mathrm{h}}(z,\hat{z}) = \boldsymbol{\Phi}(z)\boldsymbol{u}^* = \sum_{I=1}^{n} \Phi_I(z)u(z_I), \tag{25}$$

where the shape function $\boldsymbol{\Phi}(z)$ is given by

$$\boldsymbol{\Phi}(z) = (\Phi_1(z), \Phi_2(z), \ldots, \Phi_n(z)) = \bar{\boldsymbol{p}}^{\mathrm{T}}(z)\boldsymbol{C}^{-1}(z)\boldsymbol{B}(z). \tag{26}$$

From Eq. (25), we obtain

$$u_1^{\mathrm{h}}(z) = \mathrm{Re}[\boldsymbol{\Phi}(z)\boldsymbol{u}^*] = \mathrm{Re}\left[\sum_{I=1}^{n} \Phi_I(z)u(z_I)\right], \tag{27}$$

$$u_2^{\mathrm{h}}(z) = \mathrm{Im}[\boldsymbol{\Phi}(z)\boldsymbol{u}^*] = \mathrm{Im}\left[\sum_{I=1}^{n} \Phi_I(z)u(z_I)\right]. \tag{28}$$

In the ICVMLS approximation, the trial function of a two-dimensional problem is formed with a one-dimensional basis function; therefore, its number of unknown coefficients is less than that of the trial function of the MLS approximation. In the MLS approximation, the linear basis is $\boldsymbol{p}^{\mathrm{T}} = (1, x_1, x_2)$, and three unknown coefficients are included, whereas in the ICVMLS approximation, $\bar{\boldsymbol{p}}^{\mathrm{T}} = (1, \bar{z})$, and only two unknown coefficients are included. Moreover, in terms of the quadratic basis, the MLS approximation is $\boldsymbol{p}^{\mathrm{T}} = (1, x_1, x_2, x_1^2, x_1x_2, x_2^2)$, and six unknown coefficients are included, whereas the ICVMLS approximation is $\bar{p}^{\mathrm{T}} = (1, \bar{z}, \bar{z}^2)$, and three unknown coefficients are included. In this manner, for an arbitrary point in the domain, we need fewer nodes with domains of influence that cover the point, and thus we would need fewer nodes in the whole domain.

Compared with the CVMLS approximation presented by Cheng, the ICVMLS approximation has not only all the excellent features of the former, but also a more explicit physical meaning. From the ICVMLS approximation, a distinct expression for the approximating function is obtained. Because of the adoption of the conjugated polynomial basis to form the shape function, this method has higher computational accuracy and efficiency.

3. The ICVMM for two-dimensional advection–diffusion problems

Let Ω be a two-dimensional domain bounded by Γ, which is divided into two parts, Γ^u and Γ^q, such that $\Gamma = \Gamma^u \cup \Gamma^q$, $\Gamma^u \cap \Gamma^q = \phi$. Γ^u is part of the boundary on which the Dirichlet boundary conditions are prescribed, and Γ^q is part of the boundary on which the Neumann boundary conditions are prescribed. The governing equation for two-dimensional advection–diffusion problems can be written as

$$\frac{\partial u}{\partial t} - k_1\frac{\partial^2 u}{\partial x_1^2} - k_2\frac{\partial^2 u}{\partial x_2^2} - v_1\frac{\partial u}{\partial x_1} - v_2\frac{\partial u}{\partial x_2} = f(x_1,x_2,t), \quad (x_1,x_2) \in \Omega, \tag{29}$$

with the boundary conditions

$$u(x_1,x_2,t) = \bar{u}(x_1,x_2,t), \quad (x_1,x_2) \in \Gamma^u, \tag{30}$$

$$k_1\frac{\partial u(x_1,x_2,t)}{\partial x_1}n_1 + k_2\frac{\partial u(x_1,x_2,t)}{\partial x_2}n_2 = \bar{q}(x_1,x_2,t), \quad (x_1,x_2) \in \Gamma^q, \tag{31}$$

and the initial condition

$$u(x_1,x_2,0) = u_0, \tag{32}$$

where $u(x_1,x_2,t)$ is a field function at point $\boldsymbol{x} = (x_1,x_2)$ and time t; k_i is the diffusion coefficient; v_i is the advection coefficient in the x_i direction; $f(x_1,x_2,t)$ is the source term; $\bar{u}(x_1,x_2,t)$ and $\bar{q}(x_1,x_2,t)$ are the prescribed functions on the corresponding boundaries Γ^u and Γ^q, respectively; and n_i is the outward unit normal to boundary Γ in the x_i direction.

The equivalent functional is

$$\begin{aligned}\Pi = &\int_\Omega \left[u\left(\frac{\partial u}{\partial t} - f\right)\right]\mathrm{d}\Omega \\ &+ \int_\Omega \left[\frac{1}{2}k_1\left(\frac{\partial u}{\partial x_1}\right)^2 + \frac{1}{2}k_2\left(\frac{\partial u}{\partial x_2}\right)^2\right]\mathrm{d}\Omega \\ &+ \int_\Omega \left(v_1u\frac{\partial u}{\partial x_1} + v_2u\frac{\partial u}{\partial x_2}\right)\mathrm{d}\Omega - \int_{\Gamma^q} u\bar{q}\,\mathrm{d}\Gamma.\end{aligned} \tag{33}$$

The field function u, which makes $\delta\Pi$ reach zero, is the exact solution satisfying the control equation (29) and boundary condition (31). Imposing essential boundary condition (30) by the penalty method, we obtain the modified functional as

$$\Pi^* = \Pi + \frac{1}{2}\int_{\Gamma^u} (u-\bar{u})\cdot\alpha\cdot(u-\bar{u})\,\mathrm{d}\Gamma, \tag{34}$$

where α is the penalty factor. Taking the variation of Eq. (34), we have

$$\delta\Pi^* = \delta\Pi + \int_{\Gamma^u} \delta(u-\bar{u})\cdot\alpha\cdot(u-\bar{u})\,\mathrm{d}\Gamma. \tag{35}$$

Substituting Eq. (33) into Eq. (35) yields

$$\begin{aligned}\delta\Pi^* = &\int_\Omega \delta u\cdot\frac{\partial u}{\partial t}\mathrm{d}\Omega - \int_\Omega \delta u\cdot f\,\mathrm{d}\Omega \\ &+ \int_\Omega \delta(\boldsymbol{L}u)^{\mathrm{T}}\cdot\tilde{\boldsymbol{k}}\cdot(\boldsymbol{L}u)\mathrm{d}\Omega + \int_\Omega \delta u\cdot v_1\frac{\partial u}{\partial x_1}\mathrm{d}\Omega \\ &+ \int_\Omega \delta u\cdot v_2\frac{\partial u}{\partial x_2}\mathrm{d}\Omega - \int_{\Gamma^q}\delta u\cdot\bar{q}\,\mathrm{d}\Gamma \\ &+ \int_{\Gamma^u}\delta u\cdot\alpha\cdot u\,\mathrm{d}\Gamma - \int_{\Gamma^u}\delta u\cdot\alpha\cdot\bar{u}\,\mathrm{d}\Gamma,\end{aligned} \tag{36}$$

where

$$\tilde{\boldsymbol{k}} = \begin{bmatrix} k_1 & 0 \\ 0 & k_2 \end{bmatrix}, \tag{37}$$

$$\boldsymbol{L} = \begin{bmatrix} \dfrac{\partial}{\partial x_1} \\ \dfrac{\partial}{\partial x_2} \end{bmatrix}. \tag{38}$$

In the advection–diffusion problems, the field function u is not only a function of space coordinates, but also related to time. Because the time and space domains are not coupled, we apply the ICVMM in the space domain, and the finite-difference method in the time domain.

From Eq. (27), we can obtain the following approximations:

$$\begin{aligned} u(z,t) &= \mathrm{Re}[\boldsymbol{\Phi}(z)\boldsymbol{u}(t)] = \sum_{I=1}^{n} \mathrm{Re}[\Phi_I(z)]u_I(t) \\ &= \sum_{I=1}^{n} \tilde{\Phi}_I(z)u_I(t) = \tilde{\boldsymbol{\Phi}}(z)\boldsymbol{u}, \end{aligned} \tag{39}$$

$$\begin{aligned} \frac{\partial u(z,t)}{\partial t} &= \frac{\partial}{\partial t}\sum_{I=1}^{n} \tilde{\Phi}_I(z)u_I(t) = \sum_{I=1}^{n} \tilde{\Phi}_I(z)\frac{\partial u_I(t)}{\partial t} \\ &= \tilde{\boldsymbol{\Phi}}(z)\dot{\boldsymbol{u}}, \end{aligned} \tag{40}$$

where n is the node number in the compact support domain of z, and

$$\tilde{\boldsymbol{\Phi}}(z) = (\tilde{\Phi}_1(z), \tilde{\Phi}_2(z), \ldots, \tilde{\Phi}_n(z)), \tag{41}$$

$$\tilde{\Phi}_I(z) = \mathrm{Re}[\Phi_I(z)], \tag{42}$$

$$\boldsymbol{u} = (u_1(t), u_2(t), \ldots, u_n(t))^{\mathrm{T}}, \tag{43}$$

$$\dot{\boldsymbol{u}} = \left(\frac{\partial u_1(t)}{\partial t}, \frac{\partial u_2(t)}{\partial t}, \ldots, \frac{\partial u_n(t)}{\partial t}\right)^{\mathrm{T}}, \tag{44}$$

$$\begin{aligned} \boldsymbol{L}u(z,t) &= \sum_{I=1}^{n} \begin{bmatrix} \dfrac{\partial}{\partial x_1} \\ \dfrac{\partial}{\partial x_2} \end{bmatrix} \mathrm{Re}[\Phi_I(z)]u_I(t) \\ &= \sum_{I=1}^{n} B_I(z)u_I(t) = \boldsymbol{B}(z)\cdot\boldsymbol{u}. \end{aligned} \tag{45}$$

Substituting Eqs. (39), (40), and (45) into Eq. (36) yields

$$\begin{aligned} \delta\Pi^* = {} & \int_\Omega \delta[\tilde{\boldsymbol{\Phi}}(z)\boldsymbol{u}]\cdot[\tilde{\boldsymbol{\Phi}}(z)\dot{\boldsymbol{u}}]\mathrm{d}\Omega - \int_\Omega \delta[\tilde{\boldsymbol{\Phi}}(z)\boldsymbol{u}]\cdot f\mathrm{d}\Omega \\ & + \int_\Omega \delta[\boldsymbol{B}(z)\boldsymbol{u}]^{\mathrm{T}}\tilde{\boldsymbol{k}}\cdot[\boldsymbol{B}(z)\boldsymbol{u}]\mathrm{d}\Omega \\ & + \int_\Omega \delta[\tilde{\boldsymbol{\Phi}}(z)\boldsymbol{u}]\cdot v_1\frac{\partial}{\partial x_1}\tilde{\boldsymbol{\Phi}}(z)\cdot\boldsymbol{u}\mathrm{d}\Omega \\ & + \int_\Omega \delta[\tilde{\boldsymbol{\Phi}}(z)\boldsymbol{u}]\cdot v_2\frac{\partial}{\partial x_2}\tilde{\boldsymbol{\Phi}}(z)\cdot\boldsymbol{u}\mathrm{d}\Omega \\ & - \int_{\Gamma^q} \delta[\tilde{\boldsymbol{\Phi}}(z)\boldsymbol{u}]\cdot\bar{q}\mathrm{d}\Gamma + \int_{\Gamma^u} \delta[\tilde{\boldsymbol{\Phi}}(z)\boldsymbol{u}]\cdot\alpha\cdot[\tilde{\boldsymbol{\Phi}}(z)\boldsymbol{u}]\mathrm{d}\Gamma \\ & - \int_{\Gamma^u} \delta[\tilde{\boldsymbol{\Phi}}(z)\boldsymbol{u}]\cdot\alpha\cdot\bar{u}\mathrm{d}\Gamma. \end{aligned} \tag{46}$$

To get discrete system equations, the integral terms in Eq. (46) will be analyzed as follows.

The first integral term of Eq. (46) is

$$\begin{aligned} & \int_\Omega \delta[\tilde{\boldsymbol{\Phi}}(z)\boldsymbol{u}]\cdot[\tilde{\boldsymbol{\Phi}}(z)\dot{\boldsymbol{u}}]\mathrm{d}\Omega \\ &= \delta\boldsymbol{u}^{\mathrm{T}}\cdot\left[\int_\Omega \tilde{\boldsymbol{\Phi}}^{\mathrm{T}}(z)\cdot\tilde{\boldsymbol{\Phi}}(z)\mathrm{d}\Omega\right]\cdot\dot{\boldsymbol{u}} = \delta\boldsymbol{u}^{\mathrm{T}}\cdot\boldsymbol{C}\cdot\dot{\boldsymbol{u}}, \end{aligned} \tag{47}$$

where

$$\boldsymbol{C} = \int_\Omega \tilde{\boldsymbol{\Phi}}^{\mathrm{T}}(z)\cdot\tilde{\boldsymbol{\Phi}}(z)\mathrm{d}\Omega. \tag{48}$$

The second integral term of Eq. (46) is

$$\begin{aligned} \int_\Omega \delta[\tilde{\boldsymbol{\Phi}}(z)\boldsymbol{u}]\cdot f\mathrm{d}\Omega &= \delta\boldsymbol{u}^{\mathrm{T}}\cdot\int_\Omega \tilde{\boldsymbol{\Phi}}^{\mathrm{T}}(z)\cdot f\mathrm{d}\Omega \\ &= \delta\boldsymbol{u}^{\mathrm{T}}\cdot\boldsymbol{F}^{(1)}, \end{aligned} \tag{49}$$

where

$$\boldsymbol{F}^{(1)} = \int_\Omega \tilde{\boldsymbol{\Phi}}^{\mathrm{T}}(z)\cdot f\mathrm{d}\Omega. \tag{50}$$

The third integral term of Eq. (46) is

$$\begin{aligned} & \int_\Omega \delta[\boldsymbol{B}(z)\boldsymbol{u}]^{\mathrm{T}}\cdot\tilde{\boldsymbol{k}}\cdot[\boldsymbol{B}(z)\boldsymbol{u}]\mathrm{d}\Omega \\ &= \delta\boldsymbol{u}^{\mathrm{T}}\cdot\left[\int_\Omega \boldsymbol{B}^{\mathrm{T}}(z)\cdot\tilde{\boldsymbol{k}}\cdot\boldsymbol{B}(z)\mathrm{d}\Omega\right]\cdot\boldsymbol{u} = \delta\boldsymbol{u}^{\mathrm{T}}\cdot\boldsymbol{K}\cdot\boldsymbol{u}, \end{aligned} \tag{51}$$

where

$$\boldsymbol{K} = \int_\Omega \boldsymbol{B}^{\mathrm{T}}(z)\cdot\tilde{\boldsymbol{k}}\cdot\boldsymbol{B}(z)\mathrm{d}\Omega. \tag{52}$$

The fourth integral term of Eq. (46) is

$$\begin{aligned} & \int_\Omega \delta[\tilde{\boldsymbol{\Phi}}(z)\boldsymbol{u}]\cdot v_1\frac{\partial}{\partial x_1}\tilde{\boldsymbol{\Phi}}(z)\cdot\boldsymbol{u}\mathrm{d}\Omega \\ &= \delta\boldsymbol{u}^{\mathrm{T}}\cdot\int_\Omega \tilde{\boldsymbol{\Phi}}^{\mathrm{T}}(z)\cdot v_1\frac{\partial}{\partial x_1}\tilde{\boldsymbol{\Phi}}(z)\mathrm{d}\Omega\cdot\boldsymbol{u} = \delta\boldsymbol{u}^{\mathrm{T}}\cdot\boldsymbol{G}^{(1)}\cdot\boldsymbol{u}, \end{aligned} \tag{53}$$

where

$$\boldsymbol{G}^{(1)} = \int_\Omega \tilde{\boldsymbol{\Phi}}^{\mathrm{T}}(z)\cdot v_1\frac{\partial}{\partial x_1}\tilde{\boldsymbol{\Phi}}(z)\mathrm{d}\Omega. \tag{54}$$

The fifth integral term of Eq. (46) is

$$\begin{aligned} & \int_\Omega \delta[\tilde{\boldsymbol{\Phi}}(z)\boldsymbol{u}]\cdot v_2\frac{\partial}{\partial x_2}\tilde{\boldsymbol{\Phi}}(z)\cdot\boldsymbol{u}\mathrm{d}\Omega \\ &= \delta\boldsymbol{u}^{\mathrm{T}}\cdot\int_\Omega \tilde{\boldsymbol{\Phi}}^{\mathrm{T}}(z)\cdot v_2\frac{\partial}{\partial x_2}\tilde{\boldsymbol{\Phi}}(z)\mathrm{d}\Omega\cdot\boldsymbol{u} = \delta\boldsymbol{u}^{\mathrm{T}}\cdot\boldsymbol{G}^{(2)}\cdot\boldsymbol{u}, \end{aligned} \tag{55}$$

where

$$\boldsymbol{G}^{(2)} = \int_\Omega \tilde{\boldsymbol{\Phi}}^{\mathrm{T}}(z)\cdot v_2\frac{\partial}{\partial x_2}\tilde{\boldsymbol{\Phi}}(z)\mathrm{d}\Omega. \tag{56}$$

The sixth integral term of Eq. (46) is

$$\int_{\Gamma^q} \delta[\tilde{\boldsymbol{\Phi}}(z)\boldsymbol{u}]\cdot\bar{q}\mathrm{d}\Gamma = \delta\boldsymbol{u}^{\mathrm{T}}\cdot\int_{\Gamma^q} \tilde{\boldsymbol{\Phi}}^{\mathrm{T}}\cdot\bar{q}\mathrm{d}\Gamma = \delta\boldsymbol{u}^{\mathrm{T}}\cdot\boldsymbol{F}^{(2)}, \tag{57}$$

where

$$\boldsymbol{F}^{(2)} = \int_{\Gamma^q} \tilde{\boldsymbol{\Phi}}^{\mathrm{T}}\cdot\bar{q}\mathrm{d}\Gamma. \tag{58}$$

The seventh integral term of Eq. (46) is

$$\begin{aligned} & \int_{\Gamma^u} \delta[\tilde{\boldsymbol{\Phi}}(z)\boldsymbol{u}]\cdot\alpha\cdot[\tilde{\boldsymbol{\Phi}}(z)\boldsymbol{u}]\mathrm{d}\Gamma \\ &= \delta\boldsymbol{u}^{\mathrm{T}}\cdot\left[\int_{\Gamma^u} \tilde{\boldsymbol{\Phi}}^{\mathrm{T}}(z)\cdot\alpha\cdot\tilde{\boldsymbol{\Phi}}(z)\mathrm{d}\Gamma\right]\cdot\boldsymbol{u} = \delta\boldsymbol{u}^{\mathrm{T}}\cdot\boldsymbol{K}^{\alpha}\cdot\boldsymbol{u}, \end{aligned} \tag{59}$$

where

$$\boldsymbol{K}^{\alpha} = \int_{\Gamma^u} \tilde{\boldsymbol{\Phi}}^{\mathrm{T}}(z) \cdot \alpha \cdot \tilde{\boldsymbol{\Phi}}(z) \mathrm{d}\Gamma. \tag{60}$$

The eighth integral term of Eq. (46) is

$$\begin{aligned} &\int_{\Gamma^u} \delta[\tilde{\boldsymbol{\Phi}}(z)\boldsymbol{u}] \cdot \alpha \cdot \bar{u} \mathrm{d}\Gamma \\ &= \delta\boldsymbol{u}^{\mathrm{T}} \cdot \int_{\Gamma^u} \tilde{\boldsymbol{\Phi}}^{\mathrm{T}}(z) \cdot \alpha \cdot \bar{u} \mathrm{d}\Gamma = \delta\boldsymbol{u}^{\mathrm{T}} \cdot F^{\alpha}, \end{aligned} \tag{61}$$

where

$$\boldsymbol{F}^{\alpha} = \int_{\Gamma^u} \tilde{\boldsymbol{\Phi}}^{\mathrm{T}}(z) \cdot \alpha \cdot \bar{u} \mathrm{d}\Gamma. \tag{62}$$

Substituting Eqs. (47), (49), (51), (53), (55), (57), (59), and (61) into Eq. (46) yields

$$\begin{aligned} \delta\Pi^* = \ & \delta\boldsymbol{u}^{\mathrm{T}} \cdot (\boldsymbol{C}\dot{\boldsymbol{u}} + \boldsymbol{K}\boldsymbol{u} + \boldsymbol{K}^{\alpha}\boldsymbol{u} + \boldsymbol{G}^{(1)}\boldsymbol{u} \\ & + \boldsymbol{G}^{(2)}\boldsymbol{u} - \boldsymbol{F}^{(1)} - \boldsymbol{F}^{(2)} - \boldsymbol{F}^{\alpha}). \end{aligned} \tag{63}$$

As $\delta\Pi^* = 0$, and due to the arbitrariness of $\delta\boldsymbol{u}^{\mathrm{T}}$ in Eq. (63), we can obtain the final linear system as

$$\boldsymbol{C}\dot{\boldsymbol{u}} + \bar{\boldsymbol{K}}\boldsymbol{u} = \bar{\boldsymbol{F}}, \tag{64}$$

where

$$\bar{\boldsymbol{K}} = \boldsymbol{K} + \boldsymbol{K}^{\alpha} + \boldsymbol{G}^{(1)} + \boldsymbol{G}^{(2)}, \tag{65}$$

$$\bar{\boldsymbol{F}} = \boldsymbol{F}^{(1)} + \boldsymbol{F}^{(2)} + \boldsymbol{F}^{\alpha}. \tag{66}$$

Equation (64) is a system of linear ordinary differential equations, in which the time is an independent variable. If we suppose that the time step is Δt, then using the traditional difference method for two-point boundary value problems we can establish the relationship between $u|_{t+\Delta t}$ and $u|_t$ as

$$\theta \left.\frac{\partial u}{\partial t}\right|_{t+\Delta t} + (1-\theta) \left.\frac{\partial u}{\partial t}\right|_t = \frac{u|_{t+\Delta t} - u|_t}{\Delta t}. \tag{67}$$

Solving Eq. (64) for $\frac{\partial u}{\partial t}|_{t+\Delta t}$ and $\frac{\partial u}{\partial t}|_t$ respectively, and substituting the results into Eq. (67), as $\boldsymbol{C}$ is independent of time, we obtain

$$\begin{aligned} &\left(\frac{\boldsymbol{C}}{\Delta t} + \theta\bar{\boldsymbol{K}}|_{t+\Delta t}\right)\boldsymbol{u}|_{t+\Delta t} \\ &= \left(\frac{\boldsymbol{C}}{\Delta t} - (1-\theta)\bar{\boldsymbol{K}}|_t\right)\boldsymbol{u}|_t + \theta\bar{\boldsymbol{F}}|_{t+\Delta t} + (1-\theta)\bar{\boldsymbol{F}}|_t, \end{aligned} \tag{68}$$

where θ is the time weighted coefficient, of which the different values correspond to different time difference forms. When $\theta = 1/2$, equation (68) becomes

$$\begin{aligned} &\left(\frac{2\boldsymbol{C}}{\Delta t} + \bar{\boldsymbol{K}}|_{t+\Delta t}\right)\boldsymbol{u}|_{t+\Delta t} \\ &= \left(\frac{2\boldsymbol{C}}{\Delta t} - \bar{\boldsymbol{K}}|_t\right)\boldsymbol{u}|_t + \bar{\boldsymbol{F}}|_{t+\Delta t} + \bar{\boldsymbol{F}}|_t, \end{aligned} \tag{69}$$

then the relationship between $u|_{t+\Delta t}$ and $u|_t$ is obtained. Depending on the initial condition and starting from the initial time, we solve the field function the next moment after a time step, and then the field function at any time can be obtained step by step.

4. Numerical examples

For the validation of the method described above, we present two examples. In the examples, we examine the accuracy and convergent character of the ICVMM, and also make comparisons with the EFG method based on the MLS approximation, the CVMM based on the CVMLS approximation, and the ICVMM based on the ICVMLS approximation.

The following error norm is defined as the error indicator in this paper:

$$e = \sum_{i=1}^{N} \left| \frac{u_i^{\mathrm{analy}} - u_i^{\mathrm{num}}}{u_i^{\mathrm{analy}}} \right|^2, \tag{70}$$

where N is the node number, and u_i^{analy} and u_i^{num} are the analytical and the numerical solutions at node $\boldsymbol{x}_i$, respectively.

4.1. Example 1

Consider the following advection–diffusion problem:

$$\begin{aligned} \frac{\partial u(x_1,x_2,t)}{\partial t} = \ & \frac{\partial^2 u(x_1,x_2,t)}{\partial x_1^2} + \frac{\partial^2 u(x_1,x_2,t)}{\partial x_2^2} \\ & - \frac{\partial u(x_1,x_2,t)}{\partial x_1} - \frac{\partial u(x_1,x_2,t)}{\partial x_2} + f(x_1,x_2,t), \\ & (x_1,x_2) \in \Omega = [0,1]\times[0,1], \quad t > 0, \end{aligned} \tag{71}$$

with the Dirichlet-type boundary condition

$$u(x_1,x_2,t) = t^{2+\gamma} \mathrm{e}^{x_1+x_2}, \quad (x_1,x_2) \in \partial\Omega, \quad t > 0, \tag{72}$$

and the initial condition

$$u(x_1,x_2,0) = 0, \quad (x_1,x_2) \in \Omega, \tag{73}$$

where

$$f(x_1,x_2,t) = 0.5\Gamma(3+\gamma)t^2 \mathrm{e}^{x_1+x_2}. \tag{74}$$

The analytical solution is given by

$$u(x_1,x_2,t) = t^{2+\gamma} \mathrm{e}^{x_1+x_2}. \tag{75}$$

The γ in the equations above can be any value of $0 < \gamma \leq 1$, and the meshless method developed in this paper is suitable for any γ. In the following studies, we select $\gamma = 1$ for simplicity.

To illustrate the accuracy of the proposed meshless method, we choose 11×13 regularly distributed nodes. The node distribution is shown in Fig. 1. The following parameters are employed to solve this problem: penalty factor $\alpha = 1.0 \times 10^3$ and scaling parameter $d_{\max} = 2.1$.

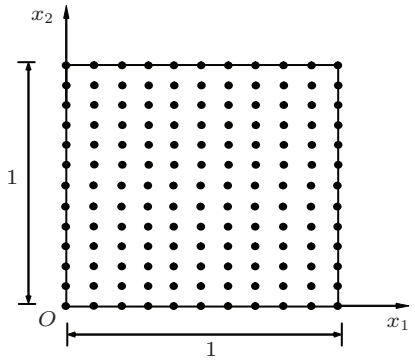


Fig. 1. Node distribution.

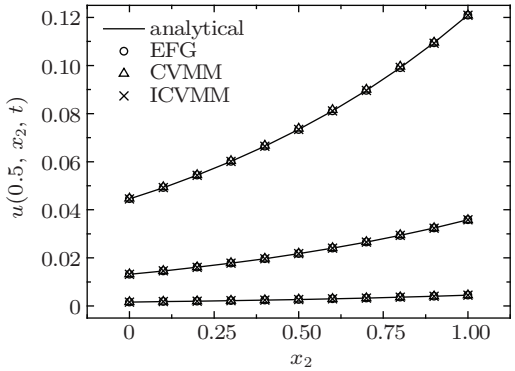


Fig. 2. Comparison of meshless methods and analytical solutions at $x_1 = 0.5$ at (from below) $t = 0.1$ s, 0.2 s, and 0.3 s.

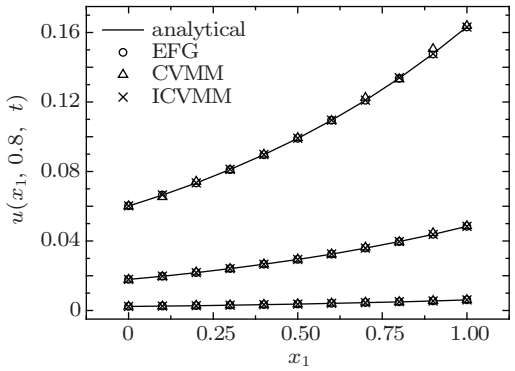


Fig. 3. Comparison of meshless methods and analytical solutions at $x_2 = 0.8$ at (from below) $t = 0.1$ s, 0.2 s, and 0.3 s.

Figures 2 and 3 present the analytical and numerical solutions obtained by the EFG method, the CVMM, and the ICVMM using different time steps at x_1 and x_2 directions, respectively. In addition, the relationship between the relative error and node number at $x_1 = 0.5$ and $t = 0.2$ s is given in Fig. 4, which shows that the solution converges as the node number increases, and the 10×10 nodes give excellent results. Moreover, the relationship between relative error and time step at $x_1 = 0.5$ and $t = 1$ s is plotted in Fig. 5, which shows that the relative error increases as the time step increases. The present results show that ICVMM not only gets excellent solutions at different times, but also has good convergent characteristics.

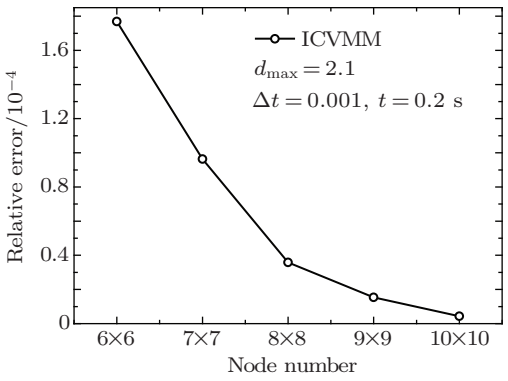


Fig. 4. The variation in total error with node number for the ICVMM.

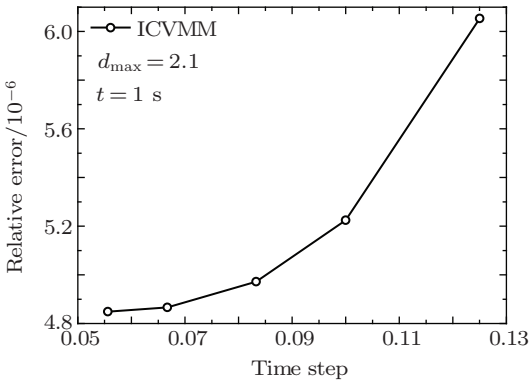


Fig. 5. The variation in total error with time step for the ICVMM.

4.2. Example 2

Consider the following advection–diffusion equation:

$$\frac{\partial u(x_1,x_2,t)}{\partial t} = k_1\frac{\partial^2 u(x_1,x_2,t)}{\partial x_1^2} + k_2\frac{\partial^2 u(x_1,x_2,t)}{\partial x_2^2} + v_1\frac{\partial u(x_1,x_2,t)}{\partial x_1} + v_2\frac{\partial u(x_1,x_2,t)}{\partial x_2},$$
$$(x_1,x_2) \in \Omega = [0,1]\times[0,1], \quad t > 0, \tag{76}$$

with the Dirichlet-type boundary conditions

$$\begin{aligned} u(0,x_2,t) &= a\mathrm{e}^{bt}(1+\mathrm{e}^{-c_2x_2}),\\ u(1,x_2,t) &= a\mathrm{e}^{bt}(\mathrm{e}^{-c_1}+\mathrm{e}^{-c_2x_2}),\\ u(x_1,0,t) &= a\mathrm{e}^{bt}(1+\mathrm{e}^{-c_1x_1}),\\ u(x_1,1,t) &= a\mathrm{e}^{bt}(\mathrm{e}^{-c_2}+\mathrm{e}^{-c_1x_1}), \end{aligned} \tag{77}$$

and the initial condition

$$u(x_1,x_2,0) = a(\mathrm{e}^{-c_1x_1}+\mathrm{e}^{-c_2x_2}), \quad (x_1,x_2) \in \Omega. \tag{78}$$

The analytical solution is given by

$$u(x_1,x_2,t) = a\mathrm{e}^{bt}(\mathrm{e}^{-c_1x_1}+\mathrm{e}^{-c_2x_2}), \tag{79}$$

where

$$c_1 = \frac{v_1+\sqrt{v_1^2+4bk_1}}{2k_1}, \tag{80}$$

$$c_2 = \frac{v_2+\sqrt{v_2^2+4bk_2}}{2k_2}. \tag{81}$$

This example is solved using the EFG method, the CVMM, and the ICVMM with a total of 143 regularly distributed nodes. The penalty factor is $\alpha = 1.0 \times 10^3$, and the scaling parameter is $d_{\max} = 2.9$.

We set $k_1 = 1.4$, $k_2 = 1.7$, $v_1 = v_2 = 1$, and $a = b = 1$ for simplicity. Figure 6 presents the analytical and the numerical solutions obtained by the three meshless methods at $x_1 = 0.2$ and $t = 0.1$ s. The ICVMM takes 12.36 s with $e = 2.79 \times 10^{-6}$, while the EFG method and the CVMM take 27.54 s and 12.45 s with $e = 7.29 \times 10^{-6}$ and $e = 2.17 \times 10^{-4}$, respectively. The ICVMM has greater computational precision than the EFG method and the CVMM, and the ICVMM and CVMM have greater computational efficiencies than the EFG method.

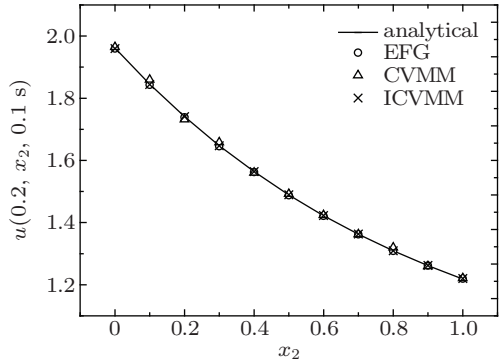


Fig. 6. Comparison of meshless methods and analytical solutions at $x_1 = 0.2$.

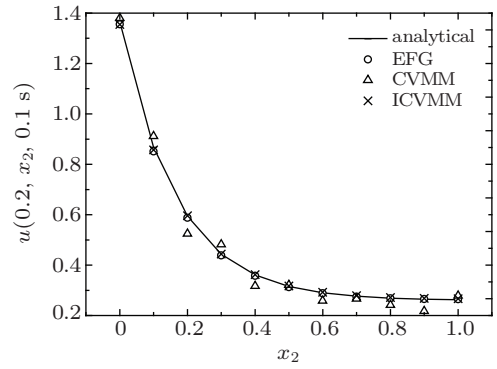


Fig. 7. Comparison of meshless methods and analytical solutions at $x_1 = 0.2$.

An extensive investigation of this example is made by considering many of the different values of the advection and diffusion coefficients. We observe that the CVMM becomes unstable for the advection dominated cases, whereas the other two methods are in excellent agreement with the analytical solutions not only for the diffusion dominated cases but also for the advection dominated ones. In order to clearly demonstrate this, we present the analytical and the numerical solutions obtained by the three meshless methods in Fig. 7, which differs from Fig. 6 by taking $v_1 = v_2 = 10$. Although the relative errors of the EFG method and the ICVMM are almost the same, the CPU time of the former is twice that of the latter. Moreover, it is clearly shown in Fig. 8 that the disagreement between the analytical solutions and the three meshless methods becomes unclear as time increases. Again, the ICVMM has better computational efficiency than the EFG method.

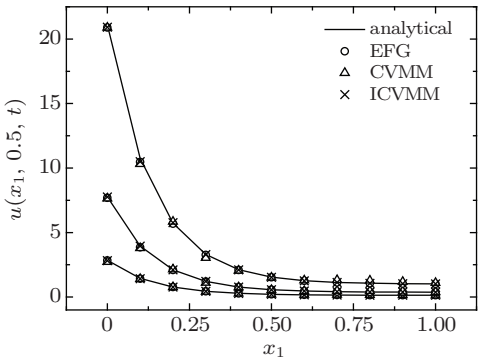


Fig. 8. Comparison of meshless methods and analytical solutions at $x_2 = 0.5$ at (from below) $t = 1$ s, 2 s, and 3 s.

5. Conclusion

Based on the ICVMLS approximation, we present the ICVMM for two-dimensional advection–diffusion problems. Two numerical examples with different nodal distributions are used to study the newly developed meshless method, and the stability and convergence of the ICVMM are examined numerically. The ICVMM gives excellent agreement with the exact solution, not only for the diffusion dominated cases but also the advection dominated ones, and has better accuracy than the CVMM and a better computational efficiency than the EFG method. In conclusion, the ICVMM has good potential in solving problems in engineering and science.

References

[1] Franca LP, Hauke G and Masud A 2006 *Comput. Method Appl. M.* **195** 1560
[2] Turner D Z, Nakshatrala K B and Hjelmstad K D 2011 *Int. J. Numer. Meth. Fl.* **66** 64
[3] Volker J and Petr K 2007 *Comput. Method Appl. M.* **196** 2197
[4] Volker J and Julia N 2012 *J. Comput. Phys.* **231** 1570
[5] Knopp T, Lube G and Rapin G 2002 *Comput. Method Appl. M.* **191** 2997
[6] Boztosun I and Charafi A 2002 *Eng. Anal. Bound Elem.* **26** 889
[7] Noye B J and Tan H H 1989 *Int. J. Numer. Meth. Fl.* **9** 75
[8] Ikeuchi M and Onishi K 1983 *Appl. Math. Model.* **7** 115
[9] Zerroukat M, Power H and Chen C S 1998 *Int. J. Numer. Meth. Eng.* **42** 1263
[10] Dai B D and Cheng Y M 2007 *Acta Phys. Sin.* **56** 597 (in Chinese)
[11] Zhang Z, Zhao P and Liew K M 2009 *Eng. Anal. Bound. Elem.* **33** 547
[12] Li S C, Cheng Y M and Li S C 2006 *Acta Phys. Sin.* **55** 4760 (in Chinese)
[13] Ren H P, Cheng Y M and Zhang W 2009 *Chin. Phys. B* **18** 4065
[14] Bai F N, Li D M, Wang J F and Cheng Y M 2012 *Chin. Phys. B* **21** 020204
[15] Cheng R J and Cheng Y M 2008 *Acta Phys. Sin.* **57** 6037 (in Chinese)
[16] Chen L and Cheng Y M 2010 *Chin. Phys. B* **19** 090204
[17] Cheng R J and Cheng Y M 2011 *Chin. Phys. B* **20** 070206
[18] Qin Y X and Cheng Y M 2006 *Acta Phys. Sin.* **55** 3215 (in Chinese)
[19] Zhuang P, Gu Y T and Liu F 2011 *Int. J. Numer. Meth. Eng.* **88** 1346
[20] Wang J F, Bai F N and Cheng Y M 2011 *Chin. Phys. B* **20** 030206
[21] Cheng Y M, Peng M J and Li J H 2005 *Chin. J. Theor. Appl. Mech.* **37** 719 (in Chinese)
[22] Belytschko T, Krongauz Y, Organ D, Fleming M and Krysl P 1996 *Comput. Methods Appl. Mech. Eng.* **139** 3